PHOTOSYNTHETICA 40 (2): 183-193, 2002

Chlorophyll-deficient mutant in oak (*Quercus petraea* L.) displays an accelerated hypersensitive-like cell death and an enhanced resistance to powdery mildew disease

V. REPKA

Laboratory of Molecular Biology and Virology, Research Institute of Viticulture and Enology (CRIVE), Matúškova 25, SK-833 11 Bratislava, Slovakia

Abstract

Plants of the discovered chlorophyll-deficient mutant of oak (ML) display enhanced disease resistance to the fungus *Erysiphe cichoracearum*, causal agent of powdery mildew. Quantitative imaging of chlorophyll (Chl) fluorescence revealed that the net photosynthetic rate (P_N) declined progressively in both untreated and invaded ML leaves as well as in inoculated wild-type (WT) leaves. Images of non-photochemical fluorescence quenching (NPQ) in both untreated and infected mutant leaves suggested that the capacity of Calvin cycle had been reduced and that there was a complex metabolic heterogeneity within the ML leaf. The ML mutant accumulates reactive oxygen species, ROS (H_2O_2) from the oxidative burst followed by spontaneous cell death that mimic the hypersensitive response. Reduction in pathogen sporulation on ML leaves correlated with the accumulation of soluble saccharides and a more rapid induction of defence responses including expression of some defence proteins (β-1,3-glucanase and chitinase). Unlike to WT plants, ML-conferred phenotype activates and/or de-represses multiple defence responses, making them more easily induced by pathogens.

Additional key words: chlorophyll fluorescence; gene expression; hypersensitive reaction; photosynthesis; programmed cell death; proteins; reactive oxygen species; sugars.

Introduction

Pathogens deploy one of three main strategies to attack plant hosts: necrotrophy, biotrophy, or hemibiotrophy. Unlike to necrotrophs that first kill host cells and then metabolise their contents, biotrophic and hemibiotrophic pathogens invade living cells and re-program metabolism to favour their growth and reproduction (Agrios 1988). Currently there is evidence that photosynthesis is a target of pathogenesis. Inhibition of photosynthetic electron transport was found in the chloroplasts of infected cells of NN tobacco leaves inoculated with tobacco mosaic virus (Seo *et al.* 2000). In addition, many rust and powdery mildew fungi cause in infected leaves a progressive decline in the rate of photosynthesis, an increase in invertase activity, and an accumulation of hexose sugars (and sometimes sucrose) (Farrar and Lewis 1987, Scholes 1992, Chou *et al.* 2000). Recently a model linking these metabolic symptoms has been proposed (Scholes 1992, Scholes *et al.* 1994). According to the model, an increase in invertase activity leads to an accumulation of soluble saccharides, and/or to a change in the flux through these metabolic pathways. This in turn promotes a signal transduction pathway(s) leading to a repression of photosynthetic gene expression and hence to a decline in the rate of photosynthesis in infected leaves. At the same time, genes required for defence responses are induced (Herbers and Sonnewald 1998). Results from studies of several host/pathogen systems have implicated accumulation or depletion of sugars in resistance to fungal infection (Van der Plank 1984). More recently, Salzman *et al.* (1998) showed that hexoses could enhance the anti-fungal

Received 11 February 2002, *accepted* 16 April 2002.
Fax: (+421) 254 775436; e-mail: vrepka@vuvv.sk
Abbreviations: Chl – chlorophyll; DAB – 3',3'-diaminobenzidine; DAI – day after inoculation; FM – fresh mass; HR – hypersensitive reaction; NPQ – non-photochemical quenching; PCD – programmed cell death; PR – pathogenesis-related; PS – photosystem; RH – relative humidity; ROS – reactive oxygen species; WT – wild type; Φ_{II} – proportion of absorbed radiation flowing through PS2.
Acknowledgements: I thank Drs. Johan Memelink, Huub J.M. Linthorst, and Imre E. Somssich for providing PR-1, -2, -3, and PAL clones, respectively. Mrs. Irma Fischerová is gratefully acknowledged for her expert technical assistance. This work was supported in part by the grant No. 27-19/STP from the Slovak Ministry of Agriculture.

efficacy of some defence-related grape proteins during berry ripening. In general, co-ordinate accumulation of anti-fungal proteins and hexoses appears to constitute a novel, developmentally regulated defence mechanism against plant pathogens.

Biochemical and physiological approaches have delivered limited progress in unravelling the cascade of events involved in the activation and regulation of defence responses. The complexity of mechanism and the probable interactions with other plant regulatory and biosynthetic pathways (*e.g.* hormones) and the environment (*e.g.* irradiance, osmotic stress, nitrogen, phosphate supply, *etc.*) make it impracticable to dissect the pathway based solely on such approaches. To ascribe a function to each induced defence response, two complementary molecular genetic approaches can be undertaken. First, targetted loss-of-function can be achieved by constitutive anti-sense suppression, co-suppression, or transposon tagging to eliminate one or all members of a particular defence gene family. Second, non-targeted mutagenesis followed by screening for disease-sensitive and/or disease-resistant mutants provide powerful tools for identification of other genes required for disease resistance. Such mutants, especially in *Arabidopsis thaliana*, are already proving useful in dissecting the contribution of various defence responses and signalling pathways to resistance (Glazebrook *et al.* 1997, Hammond-Kosack and Jones 1997, Sticher *et al.* 1997).

To better understand how plant resists the fungal pathogen *Erysiphe cichoracearum*, I isolated a naturally occurring, chlorophyll-deficient mutant of oak. By comparison with wild-type plants the mutant shows high resistance to powdery mildew and constitutive activation of several defence-related markers.

Materials and methods

Plants: Seeds of wild-type oak plants (*Quercus petraea* L.) were sown in sterile quartz sand. Two-week-old seedlings were transferred to 100 cm^3 pots containing a sand and potting soil mixture that had been autoclaved twice for 1 h. Plants were cultivated in a growth chamber with a 16-h day (95 μmol m^{-2} s^{-1} at 25±1 °C) and 8-h night (20±1 °C) cycle and 60 % relative humidity (RH). Plants were watered on alternate days and were once a month fertilised with *Substral* (*Henkel AS*, Bratislava, Slovakia).

The spontaneous Chl-deficient mutant line (ML) was selected by sequential screening of the oak nursery located near to the CRIVE campus. The conditions for cultivation and maintenance of mutant plants were the same as described for the wild-type ones.

Inoculation of plants with a pathogen: Strain CRIVE-01 of *E. cichoracearum* was maintained either on 1-year-old plants of oak (*Q. petraea* L.) or on 2-month-old tobaccos (*Nicotiana tabacum* L. cv. White Burley) by brushing diseased plants onto new plants. The conidia were sprayed on oak leaves using the *KenAir* duster (*Kenro*, Swindon, UK) and treated plants were transferred to the controlled environment (24±1 °C, RH 60 %, 16-h photoperiod at 95 μmol m^{-2} s^{-1}). Control experiment was carried out by spraying on the leaves sterile distilled water instead of the conidia inoculum.

Chl *a* and *b* contents were measured spectrophotometrically by the method of Lichtenthaler (1987). Chls were extracted with acetone, and absorbance was recorded at 664 and 647 nm using a *Shimadzu UV-1601* spectrophotometer (*Shimadzu*, Tokyo, Japan).

Photosynthesis measurements: P_N was measured with the portable photosynthesis system (model *LI-6400*, *LI-COR*, Lincoln, USA) on fully expanded leaves under the following conditions: 300 μmol m^{-2} s^{-1}, 1 000 cm^3 m^{-3} CO_2, 15 °C, and 75 % RH. The changes in Chl fluorescence were measured at 15 °C with a Chl fluorometer (*Mini PAM*, *Walz*, Effeltrich, Germany). The minimum fluorescence yield (F_0) was determined after a 30-min dark adaptation followed by irradiating the sample with a weak measuring irradiance (approximately 0.12 μmol m^{-2} s^{-1}). Thereafter, the actinic irradiance was increased step-wise up to a maximum of 1 450 μmol m^{-2} s^{-1} to determine the maximal fluorescence yield (F_m). The maximal quantum yield of photosystem 2, PS2 (F_v/F_m) was determined from the following equation:

$$F_v/F_m = F_m - F_0/F_m.$$

Simultaneous measurement of P_N and Chl fluorescence imaging were performed basically as described in Rolfe and Scholes (1995). Mutant and wild-type leaves were removed from plants just prior to use and placed in the chamber of an IRGA (*LCA-4* with *PLCA4* leaf chamber; *Analytical Development Co.*, Hoddesdon, UK) set to record CO_2 assimilation every 30 s. The CO_2 concentration was maintained at 340 μmol m^{-2} s^{-1} with 60 % RH. The leaf was maintained in darkness for 5 min. During this period an image was captured representing zero fluorescence. The leaf was then exposed to a 1.5-s pulse of saturating radiation and an image of Chl fluorescence captured. The digital images were processed using a *PhotoShop v.5.0* software (*Adobe Systems*, San José, USA).

Analysis of soluble saccharides and starch: Leaf discs (1 cm^2) were harvested from untreated and infected regions of six mutant or wild-type plants 6 h into the photoperiod, 0, 5, 10, 20, and 40 DAI. Soluble saccharides were extracted in buffered 80 % ethanol (50 mM Hepes-

NaOH, pH 7.5, 5 mM $MgCl_2$) at 70 °C. The determination of glucose, fructose, and sucrose was performed by enzyme-linked assay as described in Scholes *et al.* (1994). Leaf discs remaining after the extraction of soluble saccharides were washed in distilled water and then ground in 0.5 M Mes buffer (pH 4.5) containing 14 U of amyloglucosidase and 0.4 U of α-amylase (*Sigma*, Deisenhofen, Germany). The samples were agitated overnight at room temperature. An aliquot (0.05 cm^3) was then assayed for glucose as described in Scholes *et al.* (1994).

In situ histochemical visualisation of starch was performed using a method described by Repka and Fischerová (1999). Areas of the leaf containing starch turned black. In order to obtain semi-quantitative contents of starch in the different regions, leaves were imaged by placing them on a light box and capturing an image using a colour CCD camera (model *Progressive3*, *Sony*, Tokyo, Japan). The intensity of staining along a 2.5 cm transect was measured using the *SigmaScanPro 3* image analysis package (*SPSS*, Erkrath, Germany).

Determination of reactive oxygen species (ROS): Frozen leaves (0.5 g) were homogenised with 1 cm^3 of 0.2 M $HClO_4$ in a pre-cooled mini-mortar (*Kontes*, Vineland, USA). The extract was held on ice for 5 min and centrifuged at 10 000×*g* for 10 min at 4 °C. The supernatant was collected and either processed immediately or quick-frozen at –80 °C until further analysis. All analysis was completed within 72 h of extraction, a period in which no substantial auto-oxidation of H_2O_2 was observed. The acidic supernatant was neutralised to pH 7.0 to 8.0 with 0.2 M NH_4OH (pH 9.5) and briefly centrifuged at 3 000×*g* for 2 min to sediment the insoluble material. The coloured components in the extract were removed by applying the extract (0.5 cm^3) to a 2 cm^3 column of *AG 1X-8* resin (*Bio-Rad*, Hercules, USA) and eluting with 3 cm^3 of de-ionised water. Generation of H_2O_2 was monitored by chemiluminescence from the ferricyanide-catalysed oxidation of luminol (*Sigma*, Deisenhofen, Germany) as described by Schwacke and Hager (1992). The luminescence was detected over a 30 s period with a luminometer (model *FB12*, *Berthold*, Pforzheim, Germany). H_2O_2 contents were obtained by calibrating the counts to a standard curve generated with known amounts of H_2O_2 treated essentially as described above.

***In vivo* detection of H_2O_2 in excised leaves**: H_2O_2 was histochemically detected in the leaves of plants by using 3,3′-diaminobenzidine (DAB) as substrate (Thordal-Christensen *et al.* 1997). Briefly, leaves were excised at the base of stems with a razor blade and supplied through the cut petioles with a 1 g m^{-3} solution of DAB (pH 3.8) for 8 h under light at 25 °C. Immediately after the treatment, the leaves were immersed in boiling ethanol (96 %) for 10-30 min. This treatment decolourised the leaves except for the deep brown to black polymerisation product produced by the reaction of DAB with H_2O_2. After cooling, the leaves were extracted at room temperature in 96 % ethanol. For video-documentation, leaves were first partially re-hydrated in water, and then scanned using a flat-bed colour scanner (*ScanJet 3200 C*, *Hewlett-Packard*, Palo Alto, USA).

Alternatively, a highly sensitive fluorescent detection of H_2O_2 for *in situ* purposes was performed as follows. Intervein areas of oak leaves previously inoculated with a pathogen or control were injected with 0.4 mM 2′,7′-dichlorofluorescein diacetate (*Calbiochem*, Zug, Switzerland) at different times after inoculation. The fluorescence intensities of the fluorescent 2′,7′-dichlorofluorescein in control and inoculated leaves were observed using a video imaging-intensified cooled colour CCD camera (model *Progressive 3*, *Sony*, Tokyo, Japan) set to longer integration times. Analysis of images was performed using the *Adobe PhotoDeluxe* software (*v.2.0*, *Adobe*, San José, USA).

Histochemistry and microscopy: Methods described by Dietrich *et al.* (1994) were used for the detection of cells undergoing cell death and auto-fluorescent materials in oak leaves. Briefly, leaves were cleared by boiling in lactophenol and rinsed first in 50 % ethanol and then in water. The cleared leaves were examined for the presence of non-transparent cells. For trypan blue staining, the leaves were first boiled in lactophenol containing 0.01 % trypan blue for 10 min and then sequentially rinsed in 50 % ethanol and water. The cleared leaves were examined with a light stereomicroscope *SZX 12* (*Olympus*, Tokyo, Japan) equipped with a digital *C3030 Camedia* camera (*Olympus*, Tokyo, Japan). To visualise auto-fluorescence materials, the leaves were cleared as above and examined with a UV epifluorescence microscope *Provis AX-70* (*Olympus*, Tokyo, Japan). Images were obtained using a CCD *Progressive 3* camera (*Sony*, Tokyo, Japan) coupled to the microscope. The digital images were pseudo-coloured using the software *Adobe PhotoDeluxe 2.0* (*Adobe*, San José, USA) and printed using a photography-quality colour printer *DeskJet 930C* (*Hewlett-Packard*, Palo Alto, USA).

Spore lifting procedure: To monitor the extent of the leaf colonisation by the fungus a simple and reliable spore lifting procedure was developed. Briefly, at different time points after inoculation, the leaves were carefully covered with a piece of black self-adhesive *Scotch* tape and gently pressed for 10 s. Then the leaves were removed with forceps and the tape containing spores was fixed on a glass microscopic slide to avoid eventual loss of spores during handling. Finally, this montage was scanned using a high-resolution photographic scanner *PhotoSmart S20* (*Hewlett-Packard*, Palo Alto, USA) and digital images were processed using the software *Adobe PhotoDeluxe 2.0* (*Adobe*, San José, USA).

Northern blot analysis of photosynthetic and defence genes: Total RNA was isolated from samples (approximately 500 mg FM) harvested from control and inoculated leaves kept at –20 °C in RNA*Later* reagent (*Ambion*, Houston, USA). For Northern blot analysis, 5 μg of total RNA from each sample was separated by denaturing electrophoresis through 1.2 % agarose gels containing formaldehyde. The RNA was transferred to a nylon membrane (*TotalBlot*$^+$, *Amresco*, Solon, USA) by vacuum blotting device (*Bio-Rad*, Richmond, USA) in 10× SSC buffer (1.5 M NaCl, 0.15 M sodium citrate, pH 7.0) and then immobilised by UV cross-linking. Membranes were routinely stripped for re-probing using the *Strip-EZ* technology (*Ambion*, Houston, USA).

Non-radioactive DNA probes were prepared using a *BrightStar* psoralen-biotin labeling kit (*Ambion*, Houston, USA) according to the manufacturer's recommendations. Gene-specific probes encoding tobacco acidic PR-1 (pCNT3), PR-2 (pCI121), PR-3 (pTACH-8) proteins (Memelink *et al.* 1990), parsley PAL (pPcPAL, Somssich *et al.* 1989), and an expressed sequence tag for the small subunit of ribulose-1,5-bisphosphate carboxylase/oxygenase (*rbcS*, *Genbank I.D.* T04228) were used. The *cab1* probe is a 42-base synthetic oligonucleotide modified at the 5′-end with biotin (*Interactiva Biotech*, Ulm, Germany) derived from the *cab1* mRNA leader region, 5′-CAGCACAAAGTAAACGTTTAAGATTTG TTGTTGT-AAGCCAA-3′ (Genoud *et al.* 1998). The membranes were pre-hybridised, hybridised, and washed as described in Repka *et al.* (2000). The signal was visualised using enhanced chemiluminescence and the level of transcript accumulation was directly determined on films by area integration using a *MD 300A* computing densitometer (*Molecular Dynamics*, Sunnyvale, USA).

Unless otherwise stated, the experiments were repeated in three independent series and showed qualitatively the same results. A representative set of data is presented.

Results

Phenotype of mutants under normal growth conditions: Natural powdery mildew-resistant plants of oak were recently discovered by screening the collection growing in the nursery. Individuals derived from seeds of the resistant plants inherited a mutant (ML) phenotype, easily distinguished from their wild-type (WT) counterparts. Leaves of ML plantlets appeared pale yellow-green, especially in contrast to residual darker green tissue around the veins (Fig. 1*A*). This colour phenotype was maintained as the leaves matured and did not change with irradiance.

Light microscopic analysis of leaf sections of the same age prepared from both WT and ML plants had revealed some striking differences (Fig. 1*B*, *top panels*). In controls, the palisade mesophyll could be distinguished as a layer of closely packed columnar cells beneath the upper epidermis. In mutant plants, the palisade cells were more iso-diametric, with large air spaces between them, suggesting reduced cell-to-cell adhesion.

Striking differences were also observed in Chl content. Microscopic examination of Chl fluorescence showed a limited amount of the pigment present in the ML compared to a strong red fluorescence of WT leaves (Fig. 1*B*, *lower panels*). Quantitative analysis confirmed the overall deficiency of both Chl *a* and *b* in ML line and the total Chl content was 20 % ($p< 0.001$) of that in equivalent WT leaf (Fig. 1*C*).

Effect of pathogen inoculation on photosynthesis in ML and WT leaves: To examine the effect of powdery mildew on photosynthetic induction, leaves of 20 DAI were irradiated at 93 μmol m^{-2} s^{-1} for 1 240 s. Images of Φ_{II} and NPQ (non-photochemical quenching) were captured during this induction process (for representative images of selected time-points see Fig. 1*D*). In control WT leaves, Φ_{II} increased relatively rapidly and reached a steady-state value of 0.8 after 600 s. This corresponded to a steady-state P_N of approximately 4 μmol m^{-2} s^{-1}. In infected WT leaves, the steady-state value of Φ_{II} was not significantly different from that of non-inoculated leaves but the pattern observed during induction was more complex. The infected leaves showed three distinct regions. In the infected region, where spores were visible on the leaf, Φ_{II} was induced more slowly than other parts of the leaf. Surrounding this was a zone 2-3 mm wide, where Φ_{II} was induced very rapidly when compared with control leaf and other regions of the inoculated leaf. The non-infected part of the leaf behaved in the same way as the control leaf. The induction of NPQ ($\Delta F_m/F_m'$) was also complex. In the control WT leaf, NPQ exhibited an initial transient increase but then declined to a uniform low value. This transient increase in NPQ was greater in infected region but the final value of NPQ attained was lower. The induction of NPQ in non-infected region was similar to that of control WT leaves, although there was a slight difference in the time taken to reach a steady-state value. The similarity of images for NPQ in both control and infected WT leaves indicated that powdery mildew had not caused photodamage in any region of the leaf. Moreover, NPQ was elevated in regions where Φ_{II} was reduced, indicating that photons that were not used for photosynthetic electron transport were lost by non-photochemical process.

A distinct situation was observed when the same measurements were performed in both control and infected leaves of ML plants. In control and infected ML plants, Φ_{II} increased more quickly than in the corresponding WT plants and reached a steady-state value of 0.8 within 50 s (Fig. 1*D*). Due to its deficiency in the Chl content both control and inoculated ML leaves showed some symp-

toms of photodamage although no visible symptoms of a pathogen spread were evident.

Photosynthesis (measured by gas exchange or imaging) remained constant in control WT leaves throughout the experiment. In contrast, there was a progressive decline in P_N by infected leaves, such that by day 20 the rate was only 33 % of the control (Fig. 1*E,F,G*). Apparently, there was a very low basal photosynthetic activity in both control and infected leaves of the ML line. P_N did not change with time or irradiance except the lowest one (93 μmol m^{-2} s^{-1}).

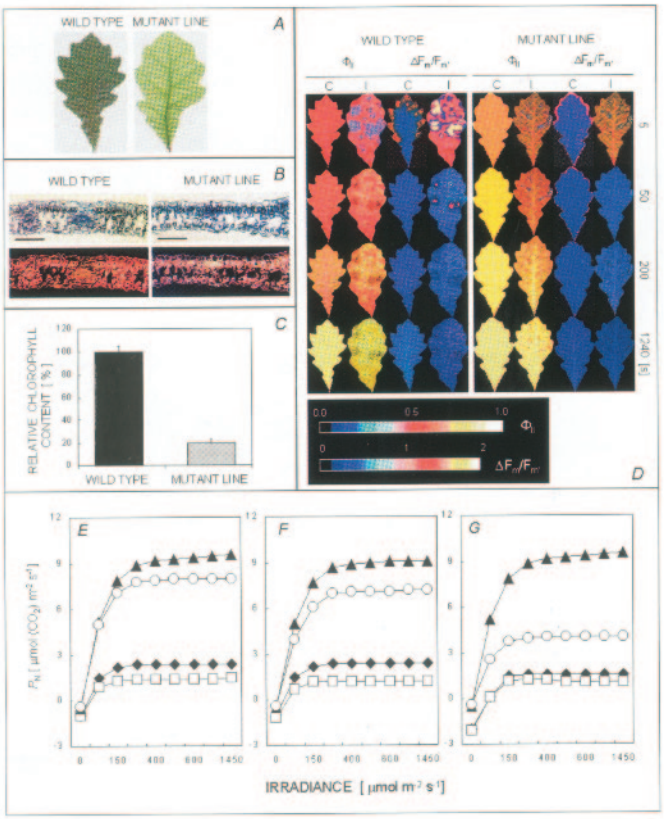

Fig. 1. Phenotypic, structural, and physiological comparisons of wild-type (WT) and mutant (ML) plants. *A*: Morphological phenotypes of leaves taken from WT and ML plants. *B*: Transverse sections of mature leaves stained with 0.1 % toluidine blue (*top panels*) or viewed under UV light (*bottom panels*). *Scale bars* equal 500 μm in all sections. *C*: Relative chlorophyll content. *Bars* indicate ± SD. *D*: Images of Φ_{II} and non-photochemical quenching ($\Delta F_m/F_m'$) for healthy (C) and infected (I) leaves of WT and ML plants. *The scales* show the relationship between colour and the relevant chlorophyll fluorescence measurement. *E*, *F*, *G*: The effect of powdery mildew on the net photosynthetic rate, P_N in leaves of WT and ML plants (*E*) 5, (*F*) 10, and (*G*) 20 DAI. Control WT (*closed triangles*), infected WT (*open circles*), control ML (*closed diamonds*), and infected ML (*open squares*).

Mutant plants display reduced disease symptoms and an accelerated cell death phenotype: The spectrum of oak responses to powdery mildew was tested by inoculating leaves of both WT and ML plants with a suspension of freshly harvested conidia under controlled environment. WT plants supported profuse asexual sporulation after 5 d (Fig. 2*A*). As demonstrated by the spore lifting technique, by 20 DAI the fungal mycelium had grown through every part of the leaf (Fig. 2*B*). Severe plant cell necrosis was apparent as early as 40 DAI (Fig. 2*A*).

In contrast, leaves of ML plants failed to support early (5 DAI) and profuse asexual sporulation characteristic of sensitive WT plants (Fig. 2*D*). Instead, these leaves showed small spontaneous patches of cell death 5 DAI, and by day 20, the entire leaf contained relatively large necrotic sectors that enlarged further with time (Fig. 2*C*).

Microscopic examination of necrotising leaves of both WT and ML plants under UV-radiation revealed a strong epifluorescence located in cells surrounding the necrotic lesions (Fig. 2*E,F*). Thus in both cases, the epifluorescence is due to the accumulation of compound derived from the phenylpropanoid pathway which is highly stimulated during a hypersensitive response (a form of programmed cell death).

Microscopic characterisation of WT and ML phenotypes: The extent of fungal development in the WT and ML plants was examined microscopically using the trypan blue stain. This was particularly informative be-

cause it not only stained fungal mycelium but was also selectively retained by necrotic plant cells and cells which had suffered membrane damage.

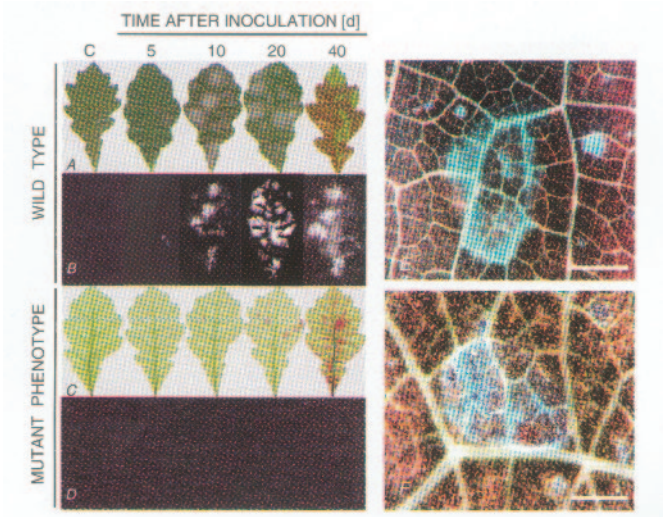

Fig. 2. Disease symptoms induced by powdery mildew strain on wild-type (WT) and mutant (ML) plants. The parental accession WT (*A*) and ML (*C*) were infected by spraying with powdery mildew conidia and photographs were taken at the indicated time points. The extent of asexual sporulation was assessed by the spore lifting technique (*B*, *D*). The leaf sections taken from WT (*E*) and ML (*F*) plants at 40 DAI were observed under UV-radiation. The blue fluorescence corresponds to an accumulation of phenylpropanoid-derived compounds. *Scale bars* equal to 100 μm in both sections.

Leaves of water-treated WT plants stained with lactophenol-trypan blue produced no obvious visible changes in their appearance (Fig. 3*A*). However, approximately 10 DAI with conidia (asexual spores) of *E. cichoracearum*, WT plants displayed abundant conidiophores (visible white powder) on mature leaves (Fig. 3*B,C*).

As shown in Fig. 3*D*, at 5 DAI with conidia ML plants displayed small scattered groups of dead cells that did not correlate with the presence of fungal structures (Fig. 3*E*). Cell death was also visible on aseptically grown ML plants (Fig. 3*F*), suggesting that the ML-conferred cell death phenotype did not depend on the presence of infectious agents. In ML leaves at 20 DAI, mycelium ingress was severely restricted within the major veins and/or to residual darker green tissue around the veins (Fig. 3*G*). The limited number of detectable spores produced appressorial germ tubes (Fig. 3*H*) that penetrated the underlying epidermal cells (Fig. 3*I*). The entire process of germination and formation of appressoria was almost completely arrested when the fungal conidia were dispersed in an unfavourable environment (Fig. 3*I*, *small arrow*).

Accumulation of ROS in ML and WT plants: Histochemical localisation of H_2O_2 using DAB in aseptically grown ML plants showed a constitutive accumulation of this ROS and the colour was visible primarily in major and to a lesser extent in minor veins of the leaves (Fig. 4*A*, *control*). Inoculation of ML plants with a pathogen increased the content of H_2O_2 in vascular tissues, as well as in cells undergoing cell death, as indicated by reddish-brown staining due to DAB polymerisation (Fig. 4*A*, *inoculated*). No substantial accumulation of H_2O_2 was histochemically detected in aseptically grown WT plants (Fig. 4*A*, *control*). Compared with control, pathogen-inoculated WT leaves showed very high rates of H_2O_2 accumulated in both vascular tissues and periveinal cells; the most intense staining was detected in cells invaded by the fungus (Fig. 4*A*, *inoculated*). A more detailed quantitative analysis of the interaction phenotypes provided results basically the same as those observed by the histochemical procedure (Fig. 4*B*).

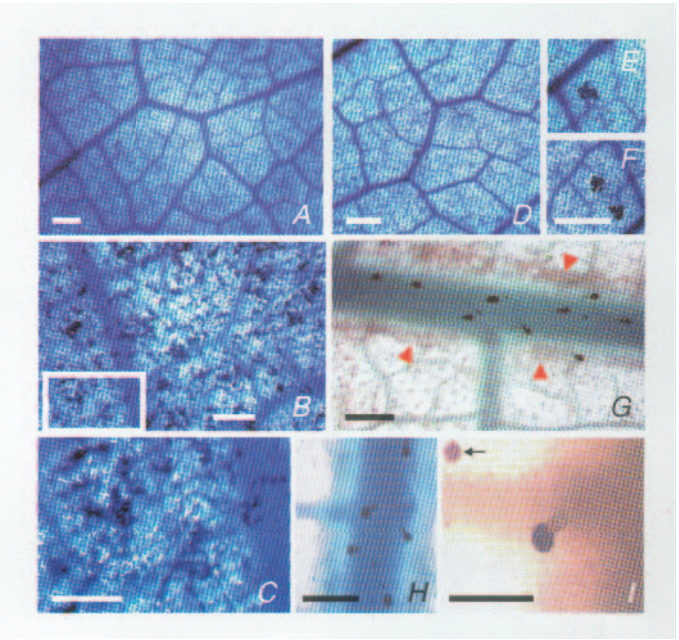

Fig. 3. Response of oak wild-type (WT) and mutant (ML) plants to *E. cichoracearum*. WT leaves stained with trypan blue at (*A*) 0 or (*B*) 10 DAI. *C*: A portion of *B* (*boxed*) showing secondary hyphae on the surface of a WT leaf at 10 DAI. ML leaves stained with trypan blue at (*D*) 0 or (*E*) 5 DAI. Note the patches of dead cells in both inoculated (*E*) and aseptically grown (*F*) ML plants. Restriction of mycelium ingress (*G*) to the major veins and to residual darker green tissue around the veins (*triangles*), attenuated formation of appressorial germ tubes (*H*) and penetration of hyphae (*I*). Note the inhibition of spore germination in an unfavourable environment (chlorophyll deficient tissues) of an ML leaf (*I*, *arrow*).

In an independent experiment, a comparative kinetic analysis of H_2O_2 formation at different developmental stages of the interaction of powdery mildew with resistant (ML) and sensitive (WT) phenotypes was undertaken. Based on analyses of fluorescence microscopy with the

fluorescent redox-sensitive dye DCFH-DA, ROS formation was triggered as soon as 1 min after inoculation of 5 d old ML leaves with a pathogen. The most intense fluorescent signal co-localised predominantly with spontaneous patches of cell death, previously revealed with trypan blue staining (Fig. 4*C*, *left panels*). Inoculated susceptible WT leaves did not produce the fluorescent dye significantly more than control leaves during this period. In contrast, a strong fluorescence could be seen in WT plants at 2 DAI when the successful penetration by the fungus was evident (Fig. 4*C*, *right panels*).

A pathogen-independent accumulation of ROS in ML plants was further demonstrated by a semi-*in vivo* test. Detached ML leaves grown on medium with DAB released a high amount of ROS, resulting in a visible change of the medium coloration which turned to dark orange (Fig. 4*D*, *left panel*). By contrast, both control and inoculated WT leaves failed in the production of a component(s) that mediate this response (Fig. 4*D*, *right panel*).

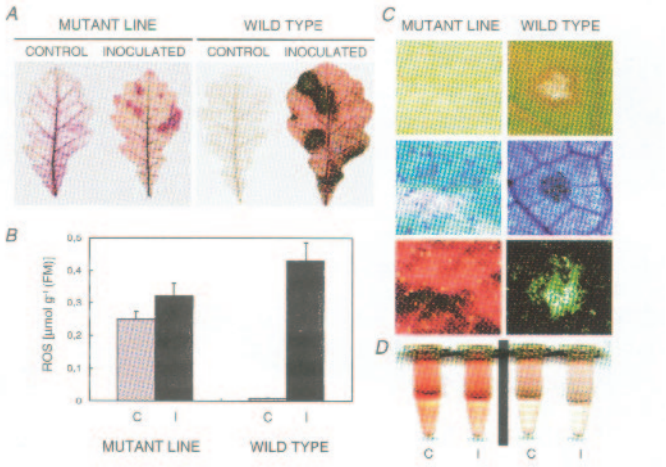

Fig. 4. Accumulation of H_2O_2 and progression of cell death in wild-type (WT) and mutant leaves. *A*: Excised leaves from untreated and inoculated WT and ML plants were supplied with a solution of DAB for 8 h, then histochemically assayed for H_2O_2. *B*: Another part of leaves treated in parallel was homogenised and the contents of H_2O_2 were monitored in the supernatant by oxidation of luminol. *Bars* indicate ±SD. *C*: The extent of cell death in both WT and ML plants (*top panels*) was assayed either with trypan blue (*middle panels*) or with a redox-sensitive probe DCFH-DA (*bottom panels*). *D*: Constitutive production of strong oxidising compound as an inherent characteristic of ML but not WT plants. C – control leaf, I – inoculated leaf.

The effect of powdery mildew on soluble saccharides and starch in ML and WT plants: In whole-leaf extract from control ML plants the amount of sucrose was much higher than in comparable leaves of WT plants (Fig. 5*A*). The basal content of sucrose was approximately four folds in ML compared with WT plants. Time course experiments revealed that starting with 10 DAI an accelerated accumulation of sucrose was detected in ML plants and it was most pronounced on day 20. There was a modest increase in the amount of sucrose in leaves of inoculated WT plants when compared with the equivalent control leaves (2-fold), but this increase was statistically significant ($p = 0.01$).

Hexoses (glucose and fructose) were barely detectable in control ML plants and the amounts of both sugars for the whole-leaf showed no correlation with the progress of infection (Fig. 5*A*). This behaviour is different from that of WT plants, in which the amounts of hexoses were dependent on both development and inoculation. The accumulation of both glucose and fructose was most pronounced on day 20.

Enzymatic analysis of the endogenous contents of starch showed that leaves of untreated ML plants had more starch than their WT counterparts (Fig. 5*B*). Upon inoculation of leaves with the pathogen the starch content was slightly higher in ML plants, while it dramatically increased in leaves of WT plants. These results were confirmed also by *in situ* assay of starch distribution (Fig. 5*C*). Starch staining at 10 DAI of WT leaves showed that the distribution of starch within the infected leaf was rather uniform but there was a darker staining sector spatially correlated with the symptoms of disease (Fig. 5*C*, *top insert*). In contrast, the pattern of starch distribution in leaves of inoculated ML plants was more complex. Beside its periveinal accumulation, the starch was predominantly localised in the vicinity of both vascular tissues and patches of cell death forming a plethora of micro-lesions (Fig. 5*C*, *bottom insert*).

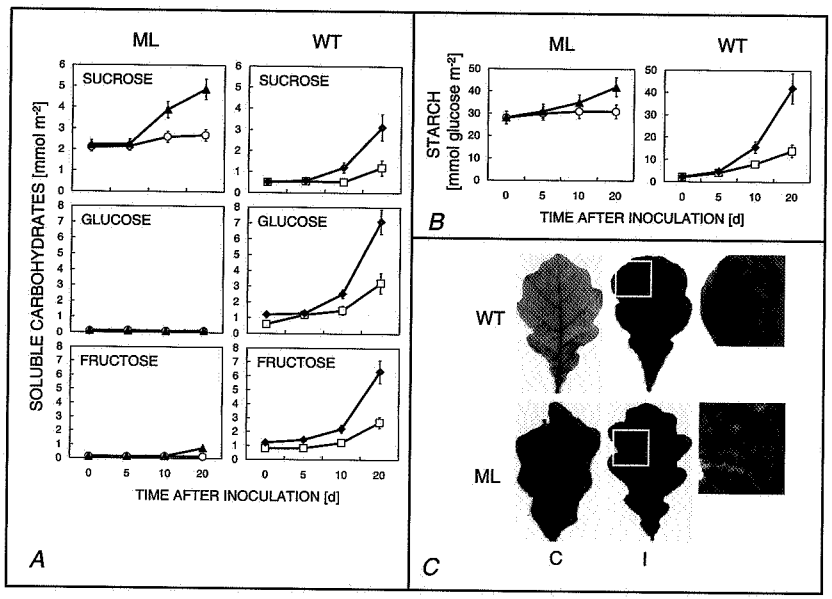

Fig. 5. The effect of powdery mildew on the amount of soluble saccharides (*A*) and on the starch content (*B*) in leaves of wild-type (WT) and mutant (ML) plants throughout the infection. Means ± SD of six replicate measurements. Infected ML (*closed triangles*), control ML (*open circles*), infected WT (*closed diamonds*), control WT (*open squares*). *C*: *In situ* starch distribution in healthy (*C*) and inoculated (*I*) WT and ML plants. Leaves harvested at the end of the night were stained with iodine solution for the presence of starch. *Inserts* represent a higher magnification (10×) of the boxed regions of inoculated WT and ML leaves to demonstrate a more detailed view of co-localisation of starch with the edge of necrotic lesions.

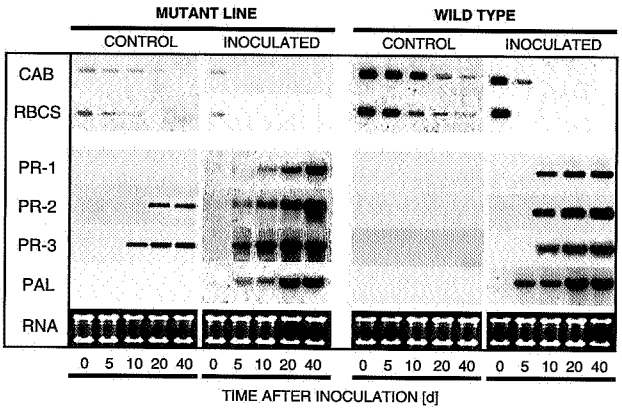

Fig. 6. Northern blot hybridisations showing the expression of genes encoding photosynthetic (CAB, RBCS) and defence-related (PR-1, PR-2, PR-3, PAL) proteins in leaves of mutant (ML) and wild-type (WT) oak plants. The ethidium bromide-stained gels (RNA) demonstrate equivalent RNA quantities loaded in each slot of the gel.

The effect of *E. cichoracearum* on the expression of genes encoding photosynthetic and defence proteins in oak leaves: As revealed by Northern blot analysis, the expression of both photosynthetic genes *cab* and *rbcS* exhibited an age-dependent decline in control leaves of ML and WT plants. The expression of these genes was repressed more profoundly upon inoculation (Fig. 6). Furthermore, the expression of both photosynthetic genes was down-regulated in the same time points when the expression of defence-related genes become up-regulated. By comparison to WT plants I observed that two (PR-2 and PR-3) of four defence genes analysed were prematurely expressed in untreated ML plants and their expression was strongly enhanced as the infection progressed. Genes encoding acidic PR-1 protein and PAL (phenylalanine ammonia-lyase) were expressed in both ML and WT plants in the same time frame although to a different extents (Fig. 6).

Discussion

I identified a novel, Chl-deficient mutant of oak that displays enhanced resistance to powdery mildew and constitutive activation of several defence-related markers. Unique features of the mutant include low basal P_N, accumulation of both sucrose and starch, production of ROS and phenylpropanoid-derived compounds, accelerated cell death phenotype, and a more rapid expression of pathogenesis-related genes. Although genetic analysis of the mutant has not been performed to date, these results suggest that the mutant may be compromised in more than one metabolic pathway.

Mutant plants had reduced Chl content in leaves and lost the ability to turn green even if grown in different photoregimes. The onset of the block of greening did not

depend on the wavelength, irradiance, and duration of irradiation. Moreover, since for Chl biosynthesis the radiation of shorter wavelength than far-red (FR) is necessary, the block of greening probably occurs during the photoperception. In *A. thaliana*, Barnes *et al.* (1996) showed that the block of greening occurs during the FR irradiation period and for these responses, *phyA* is essential (Parks and Quail 1993, Nagatani *et al.* 1993). Whether or not is the ML mutant compromised in a putative *phyA*-dependent signal transduction pathway remains to be identified.

Next to its signalling function, photons also serve as the energy source for photoassimilatory processes. Another interesting observation in this study is the increased H_2O_2 content that was detected simultaneously with a decrease in Φ_{II} and inhibition of photosynthesis in ML plants independent of pathogen inoculation. This situation may mimic the behaviour of low irradiance-adapted *Arabidopsis* plants where the use of excess photons leads to photo-oxidative stress, which causes photoinhibition, results in the inactivation of PS2 reaction centres, and reduces photosynthetic activity (Karpinsky *et al.* 1997). Obviously, under normal growing conditions plants detoxify the harmful ROS *via* very effective scavenging systems localised in both chloroplast and cytosol (Asada 1994). ML plants accumulated larger amounts of H_2O_2 than WT plants and thus failed to scavenge this ROS effectively. H_2O_2 may also have exerted direct toxic effect on the fungus. In this context, H_2O_2 has been implicated in the inhibition of the germination of spores of a number of fungal pathogens (Peng and Kuc 1992). Elevated H_2O_2 contents in ML plants may thus be responsible for initiating or promoting resistance to powdery mildew manifested at an early stage of infection. Asexual reproduction was dramatically reduced in ML plants; both the number of conidiophores formed as well as the number of conidia that make up each conidiophore were decreased. These observations suggest that the ML resistance response affects the fungus primarily before the onset of conidiophore formation.

Aside of its direct detrimental effects on pathogen, elevation of H_2O_2 content may also be responsible for initiating or promoting several other biochemical processes associated with plant disease resistance. H_2O_2 from the oxidative burst plays a pivotal role in the orchestration of a localised HR during the expression of plant disease resistance (Levine *et al.* 1994). As demonstrated in this work, sustained accumulation of H_2O_2 in leaves of ML plants coincided with the spontaneous cell death that mimics the most prominent defence response toward an attacking pathogen, *i.e.* HR. Remarkably, both the spontaneous cell death and increased resistance to *Pseudomonas syringae* were found in a dominant gain-of-function *Arabidopsis* mutant *acd6* (*a*ccelerated *c*ell *d*eath, Rate *et al.* 1999).

The photo-oxidative burst of H_2O_2 associated with photoinhibition of photosynthesis in ML plants influenced both the carbon metabolism and the defence gene activation. The leaves of ML plants accumulated large amounts of sucrose, while no glucose and fructose were found. Since these leaves also accumulated a large amount of starch it is evident that the ML mutant is not primarily compromised in sucrose metabolising pathways (invertase and sucrose synthase). Moreover, the absence of both hexoses might, at least in part, be explained by an extensive phosphorylation due to a limited demand for free hexoses. The over-expression of hexokinase (AtHXK1), which catalyses sugar phosphorylation, in transgenic *Arabidopsis* (Jang *et al.* 1997) and tomato (Dai *et al.* 1999) plants led to "sugar-sensing" phenomena that mimic the ML phenotype. These plants had reduced Chl content in leaves, very low P_N, reduced greening of cotyledons, and reduced expression of photosynthetic genes. Thus, it would be of interest to determine whether the ML mutant phenotype is affected by hexokinase.

By using an *Arabidopsis* cell culture, Oswald *et al.* (2001) showed that a block in photosynthetic electron transport with 3-(3′,4′-dichlorophenyl)-1,1′-dimethylurea prevents the increase in transcript levels of *cab* and *rbcS* that typically occurs when intracellular sugar contents are depleted. Thus, plastid-derived redox signalling can override the sugar-regulated expression of nuclear-encoded photosynthetic genes. RNA blot analyses on samples untreated or treated with a pathogen for different periods of time suggest that *cab* and *rbcS* transcript levels are inversely correlated with intracellular sucrose contents. These results are consistent with the findings from other plant systems which show that expression of nuclear-encoded photosynthetic genes is inversely correlated with intracellular soluble sugar levels (Sheen 1994, Koch 1996). Conversely, a specific set of genes is up-regulated in response to an accumulation of sugar (*the feast response*) most notably those involved in carbon storage and utilisation and in plant defence. Here, the decrease in the transcript levels for *cab* and *rbcS* genes was accompanied by expression of four defence-related genes (Fig. 6). At present, however, identity of the signal or the signal transduction pathways for the repression of photosynthetic genes and for the induction of defence genes is largely unknown. Current evidence suggests the existence of a hexokinase-dependent sugar sensing mechanism (Sheen 1994, Jang *et al.* 1997), a hexose transport associated sensor, and a sucrose-specific sensing pathway (Smeekens and Rook 1997). Only sugars that can be phosphorylated by hexokinase repressed expression of photosynthetic genes, such as *cab1* (Jang and Sheen 1994).

In addition, several reports document a causal relationship between the accumulation of H_2O_2 from the oxidative burst and induction of defence-related genes. However, the induction of PR-proteins by H_2O_2 may involve secondary signals or a slow response to chronic oxidative stress rather than a rapid, direct oxidant-mediated signal pathway (Chen *et al.* 1993, Lamb and Dixon

1997). Therefore, a major challenge for future research will be to elucidate how photosynthesis-, sugar-, and redox-derived regulatory mechanisms crosstalk to optimise disease resistance expression in response to pathogen attack.

References

Agrios, G.N.: Plant Pathology. 3rd Ed. – Academic Press, San Diego 1988.

Asada, K.: Production and action of active oxygen species in photosynthetic tissues. – In: Foyer, C.H., Mullineaux, P.M. (ed.): Causes of Photooxidative Stress and Amelioration of Defense Systems in Plants. Pp. 77-103. CRC Press, Boca Raton – Ann Arbor – London – Tokyo 1994.

Barnes, S.A., Nishizawa, N.K., Quaggio, R.B., Whitelam, G., Chua, N.-H.: Far-red light blocks greening of *Arabidopsis* seedlings via a phytochrome A-mediated change in plastid development. – Plant Cell **8**: 601-615, 1996.

Chen, Z.X., Silva, H., Klessig, D.F.: Active oxygen species in the induction of plant systemic acquired resistance by salicylic acid. – Science **262**: 1883-1886, 1993.

Chou, H.M., Bundock, N., Rolfe, S.A., Scholes, J.D.: Infection of *Arabidopsis thaliana* leaves with *Albugo candida* (white blister rust) causes a reprogramming of host metabolism. – Mol. Plant Pathol. **1**: 99-113, 2000.

Dai, N., Schaffer, A., Petreikov, M., Shahak, Y., Giller, Y., Ratner, K., Levine, A., Granot, D.: Overexpression of *Arabidopsis* hexokinase in tomato plants inhibits growth, reduces photosynthesis, and induces rapid senescence. – Plant Cell **11**: 1253-1266, 1999.

Dietrich, R.A., Delaney, T.P., Uknes, S.J., Ward, E.R., Ryals, J.A., Dangl, J.L.: *Arabidopsis* mutants simulating disease resistance response. – Cell **77**: 565-577, 1994.

Farrar, J.F., Lewis, D.H.: Nutrient relations in biotrophic infections. – In: Pegg, G., Ayers, P. (ed.) : Fungal Infections of Plants. Pp. 92-132. Cambridge Univ. Press, Cambridge 1987.

Genoud, T., Millar, A.J., Nishizawa, N., Kay, S.A., Schäfer, E., Nagatani, A., Chua, N.-H.: An *Arabidopsis* mutant hypersensitive to red and far-red light signals. – Plant Cell **10**: 889-904, 1998.

Glazebrook, J., Rogers, E.E., Ausubel, F.M.: Use of *Arabidopsis* for genetic dissection of plant defense responses. – Annu. Rev. Genet. **31**: 547-569, 1997.

Hammond-Kosack, K.E., Jones, J.D.G.: Plant disease resistance genes. – Annu. Rev. Plant Physiol. Plant mol. Biol. **48**: 575-607, 1997.

Herbers, K., Sonnewald, U.: Altered gene expression brought about by inter- and intracellularly formed hexoses and its possible implication for plant-pathogen interactions. – J. Plant Res. **111**: 323-328, 1998.

Jang, J.-C., Léon, P., Zhou, L., Sheen, J.: Hexokinase as a sugar sensor in higher plants. – Plant Cell **9**: 5-19, 1997.

Jang, J.-C., Sheen, J.: Sugar sensing in higher plants. – Plant Cell **6**: 1665-1679, 1994.

Karpinsky, S., Escobar, C., Karpinska, B., Creissen, G., Mullineaux, P.M.: Photosynthetic electron transport regulates the expression of cytosolic ascorbate peroxidase genes in *Arabidopsis* during excess light stress. – Plant Cell **9**: 627-640, 1997.

Koch, K.E.: Carbohydrate-modulated gene expression in plants. – Annu. Rev. Plant Physiol. Plant mol. Biol. **47**: 509-540, 1996.

Lamb, C.J., Dixon, R.A.: The oxidative burst in plant disease resistance. – Annu. Rev. Plant Physiol. Plant mol. Biol. **48**: 251-275, 1997.

Levine, A., Tenhaken, R., Dixon, R., Lamb, C.: H_2O_2 from the oxidative burst orchestrates the plant hypersensitive disease resistance response. – Cell **79**: 583-593, 1994.

Lichtenthaler, H.K.: Chlorophylls and carotenoids – pigments of photosynthetic biomembranes. – In: Colowick, S.P., Kaplan, N.O. (ed.): Methods in Enzymology. Vol. **148**. Pp. 350-382. Academic Press, San Diego – New York – Berkeley – Boston – London – Sydney – Tokyo – Toronto 1987.

Memelink, J., Linthorst, H.J.M., Schilperoort, R.A., Hoge, J.H.C.: Tobacco genes encoding acidic and basic isoforms of pathogenesis-related proteins display different expression patterns. – Plant mol. Biol. **14**: 119-126, 1990.

Nagatani, A., Reed, J.W., Chory, J.: Isolation and initial characterization of *Arabidopsis* mutants that are deficient in phytochrome A. – Plant Physiol. **102**: 269-277, 1993.

Oswald, O., Martin, T., Dominy, P.J., Graham, I.A.: Plastid redox state and sugars: interactive regulators of nuclear-encoded photosynthetic gene expression. – Proc. nat. Acad. Sci. USA **98**: 2047-2052, 2001.

Parks, B.M., Quail, P.H.: *hy8*, a new class of *Arabidopsis* long hypocotyl mutants deficient in functional phytochrome A. – Plant Cell **5**: 39-48, 1993.

Peng, M., Kuc, J.A.: Peroxidase-mediated hydrogen peroxide as a source of antifungal activity *in vitro* and on tobacco leaf disks. – Phytopathology **82**: 696-699, 1992.

Rate, D.N., Cuenca, J.V., Bowman, G.R., Guttman, D.S., Greenberg, J.T.: The gain-of-function *Arabidopsis acd6* mutant reveals novel regulation and function of the salicylic acid signaling pathway in controlling cell death, defense, and cell growth. – Plant Cell **11**: 1695-1708, 1999.

Repka, V., Fischerová, I.: Induction and distribution of amylolytic activity in *Cucumis sativus* L. in response to virus infection. – Acta virol. **43**: 227-235, 1999.

Repka, V., Štetková, D., Fischerová, I.: The substrate preference and histochemical localization argue against the direct role of cucumber stress-related anionic peroxidase in lignification. – Biol. Plant. **43**: 549-558, 2000.

Rolfe, S.A., Scholes, J.D.: Quantitative imaging of chlorophyll fluorescence. – New Phytol. **131**: 69-79, 1995.

Salzman, R.A., Tikhonova, I., Bordelon, B.P., Hasegawa, P.M., Bressan, R.A.: Coordinate accumulation of antifungal proteins and hexoses constitutes a developmentally-controlled defense response during fruit ripening in grape. – Plant Physiol. **117**: 465-472, 1998.

Scholes, J.D.: Photosynthesis: cellular and tissue aspects in diseased leaves. – In: Ayres, P.G. (ed.): Pests and Pathogens. Pp. 85-105. BIOS Sci. Publishers, Oxford 1992.

Scholes, J.D., Lee, P.J., Horton, P., Lewis, D.H.: Invertase: understanding changes in the photosynthetic and carbohydrate metabolism of barley leaves infected with powdery mildew. – New Phytol. **126**: 213-222, 1994.

Schwacke, R., Hager, A.: Fungal elicitors induce a transient release of active oxygen species from cultured spruce cells that is dependent of Ca^{2+} and protein-kinase activity. – Planta

187: 136-141, 1992.

Seo, S., Okamoto, M., Iwai, T., Iwano, M., Fukui, K., Isagi, A., Nakajima, N., Ohashi, Y.: Reduced levels of chloroplast FtsH protein in tobacco mosaic virus-infected tobacco leaves accelerate the hypersensitive reaction. – Plant Cell **12**: 917-932, 2000.

Sheen, J.: Feedback control of gene expression. – Photosynth. Res. **39**: 427-438, 1994.

Smeekens, S., Rook, F.: Sugar sensing and sugar-mediated signal transduction in plants. – Plant Physiol. **115**: 7-13, 1997.

Somssich, I.E., Bollmann, J., Hahlbrock, K., Kombrink, E., Schulz, W.: Differential early activation of defense-related genes in elicitor-treated parsley cells. – Plant mol. Biol. **12**: 227-234, 1989.

Sticher, L., Mauch-mani, B., Métraux, J.-P.: Systemic acquired resistance. – Annu. Rev. Phytopathol. **35**: 325-370, 1997.

Thordal-Christensen, H., Zhang, Z., Wei, Y., Collinge, D.B.: Subcellular localization of H_2O_2: H_2O_2 accumulation in papillae and hypersensitive response during the barley-powdery mildew interaction. – Plant. J. **11**: 1187-1194, 1997.

Van der Plank, J.: Sink-induced loss of resistance, high sugar disease processess and biotrophy. – In: Van der Plank, J. (ed.): Disease Resistance in Plants. 2nd Ed. Pp. 107-121. Academic Press, London 1984.